Molecular Therapy
Original Article

Transvascular Delivery of Hydrophobically Modified siRNAs: Gene Silencing in the Rat Brain upon Disruption of the Blood-Brain Barrier

Bruno M.D.C. Godinho,[1,2] Nils Henninger,[3,4] James Bouley,[3] Julia F. Alterman,[1,2] Reka A. Haraszti,[1,2] James W. Gilbert,[1,2] Ellen Sapp,[5] Andrew H. Coles,[1,2] Annabelle Biscans,[1,2] Mehran Nikan,[1,2,7] Dimas Echeverria,[1,2] Marian DiFiglia,[5] Neil Aronin,[1,6] and Anastasia Khvorova[1,2]

[1]RNA Therapeutics Institute, University of Massachusetts Medical School, Worcester, MA 01605, USA; [2]Department of Molecular Medicine, University of Massachusetts Medical School, Worcester, MA 01605, USA; [3]Department of Neurology, University of Massachusetts Medical School, Worcester, MA 01605, USA; [4]Department of Psychiatry, University of Massachusetts Medical School, Worcester, MA 01605, USA; [5]Department of Neurology, Mass General Institute for Neurodegenerative Disease, Charlestown, MA 02129, USA; [6]Department of Medicine, University of Massachusetts Medical School, Worcester, MA 01605, USA

Effective transvascular delivery of therapeutic oligonucleotides to the brain presents a major hurdle to the development of gene silencing technologies for treatment of genetically defined neurological disorders. Distribution to the brain after systemic administrations is hampered by the low permeability of the blood-brain barrier (BBB) and the rapid clearance kinetics of these drugs from the blood. Here we show that transient osmotic disruption of the BBB enables transvascular delivery of hydrophobically modified small interfering RNA (hsiRNA) to the rat brain. Intracarotid administration of 25% mannitol and hsiRNA conjugated to phosphocholine-docosahexanoic acid (PC-DHA) resulted in broad ipsilateral distribution of PC-DHA-hsiRNAs in the brain. PC-DHA conjugation enables hsiRNA retention in the parenchyma proximal to the brain vasculature and enabled active internalization by neurons and astrocytes. Moreover, transvascular delivery of PC-DHA-hsiRNAs effected *Htt* mRNA silencing in the striatum (55%), hippocampus (51%), somatosensory cortex (52%), motor cortex (37%), and thalamus (33%) 1 week after administration. Aside from mild gliosis induced by osmotic disruption of the BBB, transvascular delivery of PC-DHA-hsiRNAs was not associated with neurotoxicity. Together, these findings provide proof-of-concept that temporary disruption of the BBB is an effective strategy for the delivery of therapeutic oligonucleotides to the brain.

INTRODUCTION

Therapeutic small interfering RNAs (siRNAs) hold great promise for the treatment of genetically defined disorders by targeting disease-causing mRNAs for degradation. Chemical stabilization of siRNAs ensures potent and durable gene silencing activity,[1,2] if siRNAs can be delivered to relevant disease tissues. To date, the most advanced technology in the field consists of fully stabilized siRNAs conjugated to branched *N*-acetylgalactosamine (GalNAc), which allow for targeted delivery to hepatocytes. The success of this approach has led to several advanced clinical programs for GalNAc-conjugated siRNAs targeting liver diseases[3,4] and spurred the search for conjugates that deliver siRNAs to other tissues, including the brain.

Conjugation of lipophilic moieties has been successfully used to fine-tune biodistribution and retention of siRNAs in the brain without the need for synthetic formulation.[5–7] We have previously developed an asymmetric hydrophobically modified siRNA (hsiRNA) conjugated to phosphocholine (PC)-docosahexanoic acid (PC-DHA), the most abundant fatty acid in the brain.[6] The attachment of PC-DHA facilitates cellular uptake in neuronal cultures without affecting RNA-induced silencing complex (RISC) loading and mRNA silencing.[6] Furthermore, when locally injected in the striatum, PC-DHA-hsiRNAs display improved tissue accumulation and show broad distribution throughout the brain, producing robust gene knockdown with a favorable *in vivo* toxicity profile.[6,7] Although after intravenous injections PC-DHA-hsiRNAs present enhanced blood circulating times and reduced renal clearance when compared with unmodified siRNAs,[8] after systemic administrations this class of conjugated oligonucleotides achieves limited distribution to the CNS (delivery is mostly restricted to the choroid plexus).[6] Similarly, other therapeutic oligonucleotides, including cholesterol-conjugated siRNAs and antisense oligonucleotides (ASOs), are also unable to freely cross the blood-brain barrier (BBB) and enter the brain when delivered systemically.[9,10] Thus, despite the advances in conjugate and nucleic acid chemistry, the low permeability of this specialized biological barrier

Received 5 March 2018; accepted 3 August 2018;
https://doi.org/10.1016/j.ymthe.2018.08.005.

[7]Present address: Ionis Pharmaceuticals, San Diego, CA 92010, USA

Correspondence: Anastasia Khvorova, RNA Therapeutics Institute, University of Massachusetts Medical School, 368 Plantation Street, AS4-1049, Worcester, MA 01605, USA.
E-mail: anastasia.khvorova@umassmed.edu
Correspondence: Bruno M.D.C. Godinho, RNA Therapeutics Institute, University of Massachusetts Medical School, 368 Plantation Street, AS4-1013, Worcester, MA 01605, USA.
E-mail: bruno.godinho@umassmed.edu

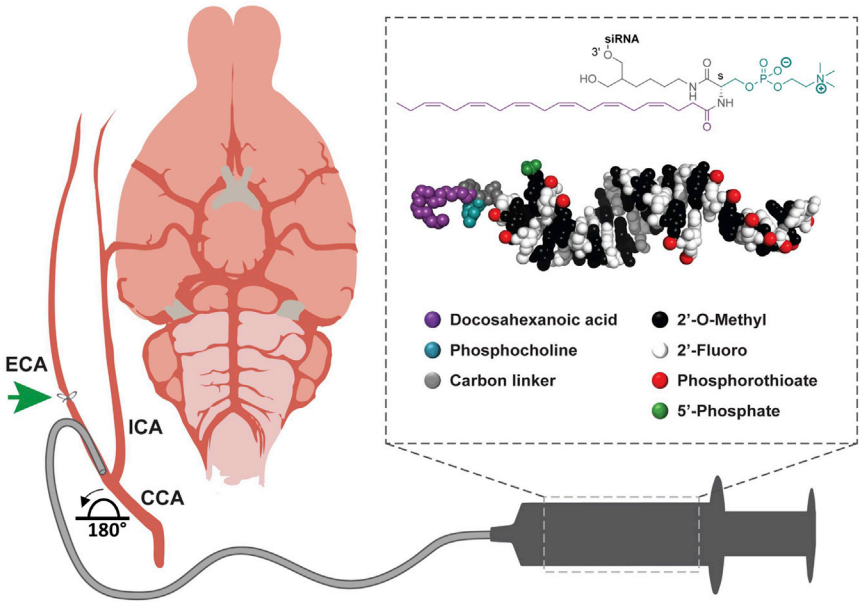

Figure 1. Blood-Brain Barrier Disruption Approach for Transvascular Delivery of PC-DHA-hsiRNAs to the Rat Brain

Schematic illustrating cannulation and intracarotid administration of mannitol and PC-DHA-hsiRNAs to the rat brain. Anesthetized rats were placed in a supine position and the carotid artery exposed at the level of the neck. The external carotid artery (ECA) was distally ligated and the cannula advanced to the bifurcation of the common carotid artery (CCA). The ECA stump was rotated ~180° to enable alignment with the proximal end of the internal carotid artery (ICA). The proximal end of the CCA was transiently clamped during injections. Mannitol (25%) was administered to disrupt the blood-brain barrier (BBB), followed by phosphocholine-docosahexanoic acid (PC-DHA) hydrophobic siRNAs (hsiRNA) 5 min after. (box, top) Chemical structure of PC-DHA. (box, bottom) PyMOL molecular model of PC-DHA-hsiRNAs. PC-DHA is conjugated to the 3′ end of the sense strand. The asymmetric siRNA is fully chemically modified with alternating 2′-O-methyl and 2′-fluoro sugar modifications and phosphorothioate backbone linkages. The antisense strand contained 5′-phosphate modification. After all injections, the proximal end of the ECA was ligated and catheters removed.

remains a primary challenge for meaningful transvascular delivery of therapeutic oligonucleotides to the brain.

Several delivery strategies have been developed to circumvent the BBB and achieve therapeutic concentrations of oligonucleotides within the CNS. Intrathecal injection (or spinal tap) is a clinically accepted way to deliver oligonucleotides via cerebrospinal fluid (CSF),[11] and allows efficient targeting in the spinal cord, but limited distribution to deeper structures of the brain.[12,13] Better delivery to these structures can be achieved by intraparenchymal or intracerebroventricular (i.c.v.) injections; however, due to their highly invasive nature and relative small dosing volumes, neither method has gained wide clinical acceptance for therapeutic delivery. To overcome some of these limitations and capitalize on the vast capillary network of the brain, approaches that aim to transiently disrupt the BBB have gained considerable attention as a way to improve transvascular delivery of therapeutics to the brain.[14]

Pharmacological disruption using hyperosmolar agents, such as mannitol, results in osmotic shrinkage of endothelial cells and opening of tight junctions, leading to a temporary disruption of the BBB.[14] Clinical trials have demonstrated the therapeutic utility of this strategy for the delivery of chemotherapeutics and monoclonal antibodies for the treatment of aggressive malignant gliomas.[15–18] In these studies, improvements on tumor response rates and patient survival were reported.[15–18] Experimentally, the ability of mannitol to temporarily disrupt the BBB has been also evaluated as a strategy for transvascular delivery of viral vectors,[19–21] nanoparticles,[22] and recombinant proteins[23] with varying degrees of success. Moreover, the only study conducted with therapeutic oligonucleotides described poor delivery of ASOs to the brain after intravenous administrations of mannitol.[9] The insufficient increase in BBB permeability after intravenous mannitol, and the fast clearance of these compounds from the blood, negatively impacted the outcome of the study. Therefore, further investigations are required to establish the value of mannitol-based strategies for transvascular delivery of therapeutic oligonucleotides to the brain.

Here we use mannitol to transiently disrupt the BBB and promote transvascular delivery of fully chemically stabilized hsiRNAs conjugated to PC-DHA. PC-DHA was selected as a model ligand for this proof-of-concept study because of its advanced features for both systemic and CNS applications. We demonstrate that cannulation of the external carotid artery (ECA) allows efficient temporal mannitol-based disruption of the BBB and productive delivery of oligonucleotide to half of the rat brain.

RESULTS

Osmotic BBB Disruption Enables Broad Transvascular Delivery of PC-DHA-hsiRNAs to the Ipsilateral Brain

Exploratory studies were conducted to test whether intracarotid administrations of mannitol in rats would lead to suitable disruption of the BBB. We monitored BBB disruption by administering Evans blue, an inert dye that binds serum albumin and is normally excluded from the brain. Multiple intravenous injections of 25% mannitol yielded negligible Evans blue dye in the brain. By contrast, after a single intracarotid administration of 25% mannitol, we observed broad ipsilateral staining with Evans blue (Figure S1), thus suggesting that intracarotid administrations of mannitol might be adequate for hsiRNA delivery to brain.

To investigate delivery of hsiRNA to the brain, we administered 25% mannitol followed by 37 mg/kg Cy3-labeled PC-DHA-hsiRNA through the right carotid artery (Figure 1). After 48 hr,

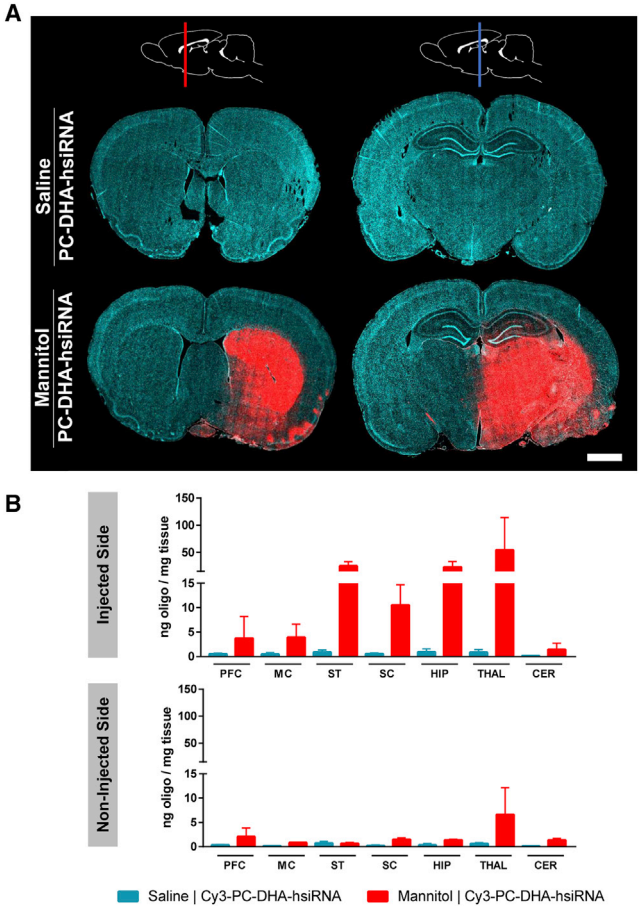

Figure 2. PC-DHA-hsiRNAs Show Widespread Distribution in the Rat Brain following Mannitol-Induced Disruption of the Blood-Brain Barrier

Cy3-labeled PC-DHA-hsiRNAs (37 mg/kg) were administered through the right carotid artery preceded by saline or mannitol, and rats were euthanized 48 hr after injections. (A) Tiled fluorescent images (20× objective) were obtained from coronal sections. The schematic at the top shows the approximate positions of the anterior (red line) and posterior (blue line) sections. Cyan: nuclei (DAPI); red: Cy3-labeled PC-DHA-hsiRNA. Scale bar, 2 mm. (B) Concentrations of PC-DHA-hsiRNA guide strands were quantified by PNA-based hybridization assay. Tissues were assayed from injected (top) and non-injected (bottom) sides of the brain. n = 2–3 animals/group, mean ± SD. CER, cerebellum; HIP, hippocampus; MC, motor cortex; PFC, pre-frontal cortex; SC, somatosensory cortex; ST, striatum; THAL, thalamus.

oligonucleotide distribution was assessed by analyzing Cy3 fluorescence in brain sections or quantifying hsiRNA guide strands in tissue punches taken from different regions of the brain. Fluorescence imaging of coronal sections of the brain revealed that Cy3-labeled PC-DHA-hsiRNAs mainly accumulate in the striatum, thalamus, and hippocampus of rats treated with mannitol, but not those rats treated with saline control (Figure 2A). Within the mannitol-treated group, a differential pattern of oligonucleotide distribution throughout the brain parenchyma was observed, suggesting that the extent of BBB disruption varied among animals. Moreover, distribution of Cy3-labeled PC-DHA-hsiRNA within the brain correlated with branching of the cerebral vascular tree: Cy3 fluorescence was highest in regions proximal to the anterior choroidal artery (AChA), middle cerebral artery (MCA), and anterior cerebral artery (ACA), in that order, and lowest near distal branches of the vascular tree. In these studies, conjugation of PC-DHA was found to be a strong determinant for oligonucleotide retention in the brain after BBB disruption. Under the same experimental conditions, Cy3-labeled siRNAs not containing the polyunsaturated fatty acid lipid moiety were rapidly cleared from the brain within 48 hr after transvascular delivery (Figure S2). Unconjugated Cy3-labeled siRNAs presented a diffused pattern of distribution in the ipsilateral brain mainly accumulating in the thalamus and hippocampus (Figure S2), but to a much lower extent to that observed for PC-DHA-hsiRNAs.

The regional distribution within the brain was confirmed by quantification of hsiRNA guide strands using a peptide nucleic acid (PNA)-based hybridization assay (Figure 2B). High levels PC-DHA-hsiRNA guide strands were detected in ipsilateral regions of the brain supplied by the right carotid system, including the striatum (25 ng hsiRNA per milligram tissue), somatosensory cortex (11 ng/mg), hippocampus (23 ng/mg), and thalamus (54 ng/mg) (Figure 2B). Low levels of PC-DHA-hsiRNA were detected in regions supplied by the superior cerebellar arteries (e.g., cerebellum; Figure 2B). Consistent with the microscopy analyses above, we detected low levels of hsiRNA guide strands in the undisrupted contralateral brain supplied by the left carotid artery (Figure 2B). Thus, carotid administration of mannitol is required for suitable osmotic disruption of the BBB and to allow efficient transvascular delivery of PC-DHA-hsiRNA to the brain parenchyma.

Animals not subjected to BBB disruption showed minimal transvascular delivery of PC-DHA-hsiRNAs to the brain (Figure 2). In agreement, intracarotid administration of a different hsiRNA conjugate, cholesterol-conjugated hsiRNAs (Chol-hsiRNA), resulted in limited distribution to the brain parenchyma (Figure S3). However, Chol-hsiRNAs were retained in non-barrier territories adjacent to the lateral and third ventricle of the injected side (Figure S3). Given its narrow therapeutic index for brain applications, transvascular delivery of Chol-hsiRNAs using mannitol was not further investigated in this study.

PC-DHA-hsiRNAs Are Internalized by Neurons and Glia after Transvascular Delivery

To examine distribution of Cy3-labeled PC-DHA-hsiRNAs at the cellular level within the brain parenchyma, we stained tissues sections with antibodies against specific neuronal (NeuN) and astroglial (glial fibrillary acidic protein [GFAP]) markers, and used DAPI to enable identification of the nucleus.

In control rats treated with saline, Cy3-labelled PC-DHA-hsiRNAs (red) were mostly detected in endothelial cells and surrounding areas in regions of the brain supplied by the right carotid vasculature, especially striatum, cortex, and thalamus (Figure 3, filled arrowheads). Although no specific marker was used to stain blood vessels in this study, these were easily identified based on the typical morphology

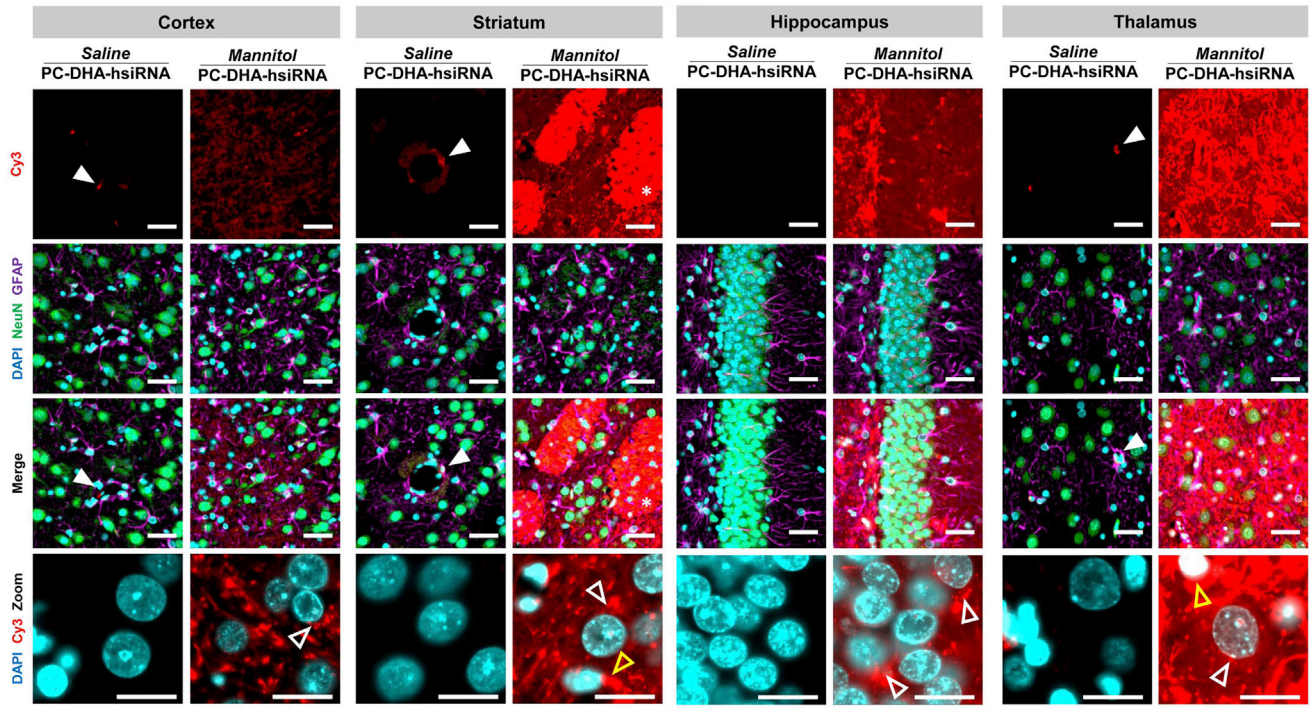

Figure 3. PC-DHA-hsiRNAs Localize to Neurons and Glia after Transvascular Delivery

Cy3-labeled PC-DHA-hsiRNAs (37 mg/kg) were administered through the right carotid artery preceded by saline or mannitol, and rats were euthanized 48 hr after injections. High-magnification (63× objective) fluorescent images were acquired from representative regions of the brain, including motor cortex (cortex), caudate putamen (striatum), thalamic nucleus (thalamus), and dentate gyrus (hippocampus). Nuclei (DAPI, cyan), astrocytes (GFAP, magenta), neurons (NeuN, green), and hsiRNAs (Cy3, red) were labeled. Filled arrowheads indicate binding to the neurovascular unit of the BBB. Unfilled arrowheads indicate perinuclear localization of PC-DHA-hsiRNAs within neurons (white arrowheads) and astrocytes (yellow arrowheads). Scale bars, 40 μm.

of the neurovascular unit. The high density of astrocyte endfeet around a blood vessel allowed straightforward identification of the vasculature present on a given field of view solely based on GFAP staining.

In rats treated with mannitol, Cy3-labelled PC-DHA-hsiRNAs (red) were detected in NeuN-positive neurons (green) and GFAP-positive astroglia (magenta) in several regions of the rat brain, including the striatum, cortex, hippocampus, and thalamus (Figure 3). In neurons and astrocytes, Cy3-labeled PC-DHA-hsiRNAs localized to the perinuclear region (Figure 3, unfilled arrowheads), but were also found in cellular processes. PC-DHA-hsiRNAs also presented a diffused pattern of distribution in the extracellular matrix in all regions analyzed. In the striatum, Cy3-labeled PC-DHA-hsiRNAs were also found to be associated with myelinated nerve bundles (Figure 3, asterisks).

Transvascular Delivery of PC-DHA-hsiRNA Supports Gene Silencing in the Rat Brain

Upon determining that mannitol-induced BBB disruption was an effective strategy for delivering PC-DHA-hsiRNA to the rat brain parenchyma, gene silencing efficacy studies were carried out. In these studies, huntingtin (*Htt*) was used as a model gene target to validate the feasibility of the approach and provide proof-of-concept. Compared with control rats injected with saline, PC-DHA-hsiRNA^{HTT} significantly reduced *Htt* mRNA levels in the striatum (55%), hippocampus (51%), somatosensory cortex (52%), motor cortex (37%), and thalamus (33%), but not in the pre-frontal cortex, cerebellum, and brainstem (Figure 4). Brain tissues that showed the greatest silencing of *Htt* mRNA received >10 ng of hsiRNA per milligram of tissue (Figure 2B) in our biodistribution studies, suggesting that the degree of knockdown correlates with the amount of hsiRNA delivered. Furthermore, these data also support the notion that the Cy3 label had a negligible impact on the pattern of distribution of this lipophilic PC-DHA-hsiRNA.

At 7 days after treatment, we detected a significant reduction of HTT protein in the thalamus (41%; $p < 0.05$; Figure 5). We also detected modest reductions of HTT protein levels in the striatum and hippocampus (Figure S4), but the changes were not statistically significant. Transvascular delivery of a non-targeting control siRNA (PC-DHA-hsiRNA^{NTC}) did not reduce *Htt* mRNA or protein levels in any brain tissue.

Mannitol Promotes Transvascular Delivery of PC-DHA-hsiRNAs without Major Acute Neurotoxic Adverse Events

Exploratory studies revealed that direct administration of mannitol and PC-DHA-hsiRNA through the common carotid artery (CCA)

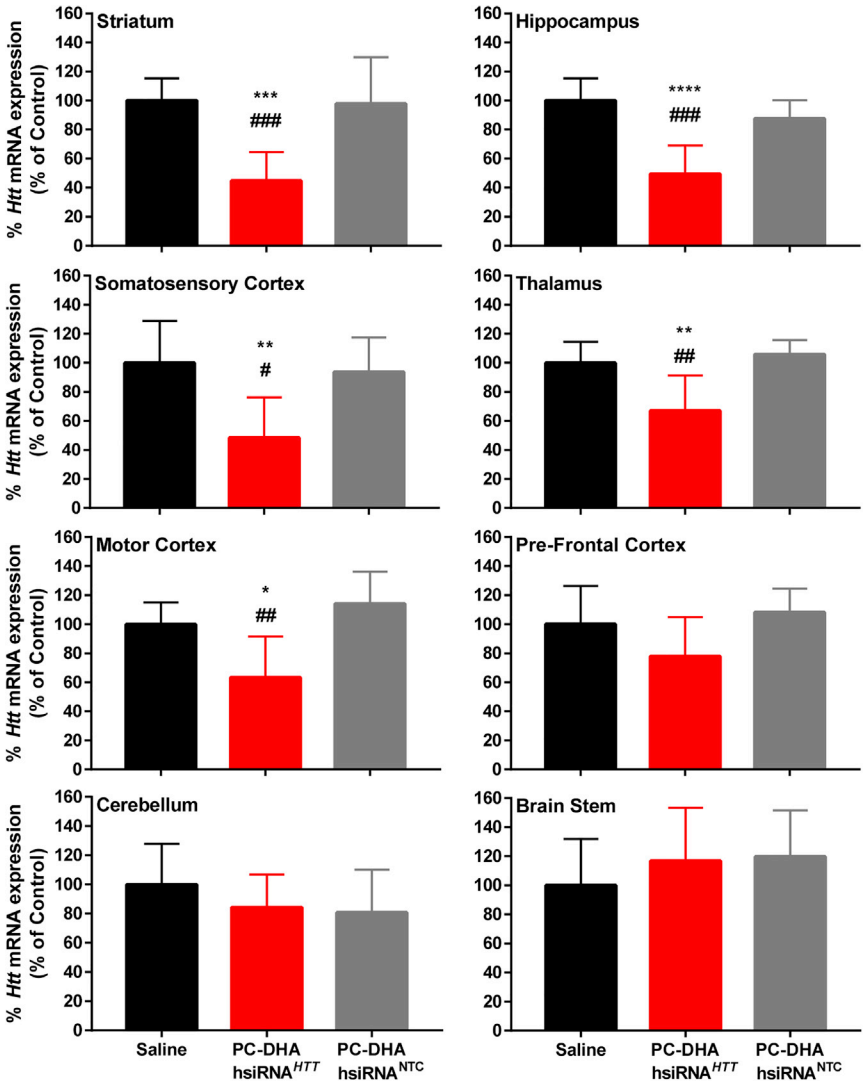

Figure 4. PC-DHA-hsiRNAs Enable Gene Silencing in Various Brain Regions after Transvascular Delivery

PC-DHA-hsiRNAs (16 mg/kg) or saline was administered through the right carotid artery after pre-treatment with mannitol. Huntingtin (HTT)-targeting (PC-DHA-hsiRNA^{HTT}) and non-targeting control (PC-DHA-hsiRNA^{NTC}) sequences were used. Gene expression was assessed from tissue punch biopsies from the injected side 7 days post-injection. Data were normalized to a housekeeping gene (cyclophilin β) and presented as a percentage of saline control. n = 7–8 animals/group, mean ± SD. One-way ANOVA with Tukey's post hoc test: *p < 0.05, **p < 0.01, ***p < 0.001, ****p < 0.0001, PC-DHA-hsiRNA^{HTT} versus saline control; #p < 0.05, ##p < 0.01, ###p < 0.001, PC-DHA-hsiRNA^{HTT} versus PC-DHA-hsiRNA^{NTC}.

with subsequent ligation of this artery resulted in increased apoptosis in the brain (Figures 6 and 7; Supplemental Materials and Methods). Thus, we chose to administer mannitol and PC-DHA-hsiRNA through an alternative method, via cannulation of the ECA. Using this indirect administration approach, we achieved high levels of delivery of PC-DHA-hsiRNAs in regions such as the striatum and thalamus without inducing major apoptosis by 48 hr (TUNEL staining; Figures 6 and 7).

In these studies, we detected an increase in GFAP in brains of rats treated with PC-DHA-hsiRNA^{HTT} 7 days post-treatment (Figure 5; Figure S4). Overall, this effect was also evident in animals treated with PC-DHA-hsiRNA^{NTC}, but not in the saline group across the regions analyzed, including the thalamus, hippocampus, and striatum (Figure 5; Figure S4). Although this suggests a transient local inflammatory response in the brain, the response was not statistically significant across groups.

Within the first day after cannulation of the ECA, all experimental and control rats lost ~10% of body mass because of the surgical procedure. After this initial weight loss, animals slowly recovered their weight, with the PC-DHA-hsiRNA^{HTT} group showing statistically significant recovery compared with control groups (Figure S5). Finally, transvascular administration of saline or PC-DHA-hsiRNA^{HTT} mildly reduced blood urea nitrogen (BUN), but blood chemistry was otherwise normal (Figure S6).

DISCUSSION

Adequate biodistribution of therapeutic oligonucleotides to the brain is essential to achieve long-lasting gene silencing effects that could improve neuropathology of patients with neurological disorders. From a clinical standpoint, transvascular delivery of therapeutic oligonucleotides to the brain represents an attractive strategy because it would allow for routine systemic administrations and eliminate the need for major neurosurgery. However, the inability to efficiently overcome the BBB has limited the potential utility of systemic administrations for CNS delivery of RNAi-based drugs.[9,24] In this study, we have shown that temporary disruption of the BBB by mannitol allows transvascular delivery of fully modified PC-DHA-hsiRNAs to the brain. The results here described establish important proof-of-concept for the use of BBB-disruption strategies for oligonucleotide delivery to the brain.

Mannitol facilitates delivery of PC-DHA-hsiRNAs to the brain through osmotic shrinkage of brain endothelial cells and transient widening of the tight junctions. In this study, intracarotid administrations allowed high concentrations of both mannitol and PC-DHA-hsiRNAs to pass through the brain vasculature before entering the venous system. This strategy resulted in broad distribution throughout the ipsilateral hemisphere of the brain, with the highest

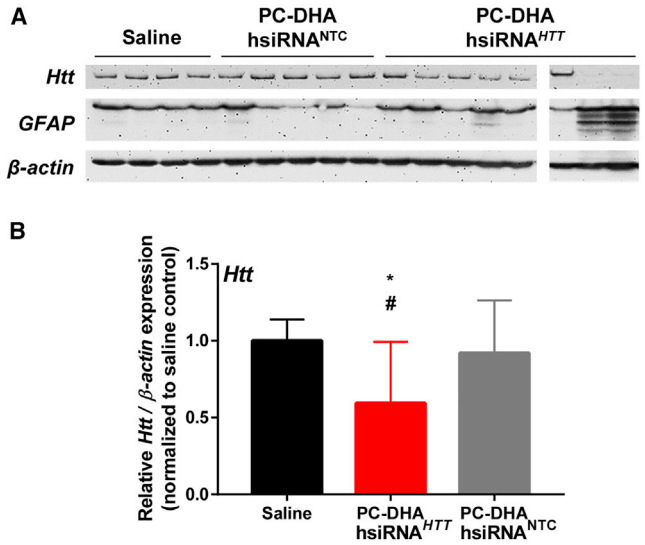

Figure 5. Transvascular Delivery of PC-DHA-hsiRNA Reduces HTT Protein in the Rat Brain

PC-DHA-hsiRNAs (16 mg/kg) or saline was administered through the right carotid artery after pre-treatment with mannitol. Huntingtin (HTT)-targeting (PC-DHA-hsiRNA^{HTT}) and non-targeting control (PC-DHA-hsiRNA^{NTC}) sequences were used. Levels of HTT and glial fibrillary acidic protein (GFAP) expression were assessed by western blots 7 days post-injection. (A) Representative blots depicting protein levels from tissue biopsies collected from the ipsilateral thalamus. (B) Densitometry analysis of HTT protein levels normalized to β-actin and expressed relatively to saline control. n = 7–8 animals/group, mean ± SD. One-way ANOVA with Tukey's post hoc test: *$p < 0.05$, PC-DHA-hsiRNA^{HTT} versus saline; $^{\#}p < 0.05$, PC-DHA-hsiRNA^{HTT} versus PC-DHA-hsiRNA^{NTC}.

degree of delivery achieved in proximal regions of the brain vascular tree. Similar patterns of delivery to the brain have been reported for inert dyes, lipid-nanoparticles, and viral vectors upon intra-arterial delivery of mannitol.[21,25,26] By contrast, intravenous administrations of mannitol followed by ASOs, or other small molecular tracers, resulted in limited delivery to the brain.[9,25] The poor transvascular delivery observed in these studies was most likely due to insufficient BBB opening and to the rapid systemic clearance of oligonucleotides after systemic administrations.[8] Therefore, the approach described here represents a significant improvement that maximizes disruption of the BBB and the concentration of oligonucleotides available at the brain vasculature for uptake.

Without BBB disruption, intracarotid injections of chemically distinct lipophilic hsiRNA conjugates (i.e., PC-DHA-hsiRNAs and Chol-hsiRNAs) revealed no significant delivery advantage. Chol-hsiRNAs were limited to territories adjacent to the lateral and third ventricle of the injected side. A similar distribution to non-barrier regions was reported for sulfatide liposomes.[26] PC-DHA-hsiRNAs noticeably bound to brain endothelial cells without significant delivery to the brain parenchyma, in agreement with a previous study showing that PC-DHA-hsiRNAs do not readily cross the BBB when administered by intravenous injection.[6] We believe that PC-DHA-hsiRNAs likely bind to brain endothelia through the Mfsd2a receptor,[27,28] the cognate receptor for lysophosphatidylcholine DHA, a highly enriched fatty acid in the brain. Perhaps inadequate Mfsd2a density for oligonucleotide uptake, or slow recycling to the cell membrane, limits the uptake of PC-DHA-hsiRNAs without mannitol treatment. Indeed, high density and rapid recycling of the asialoglycoprotein receptor in the liver are key features that enable effective delivery of GalNAc-conjugated oligonucleotides to human hepatocytes.[29] Although there are several receptor-mediated transport systems on the BBB that allow transfer of endogenous molecules, such as insulin and transferrin,[30] harnessing these systems to achieve meaningful delivery of therapeutic oligonucleotides to the brain has been proved to be challenging. In addition to the complexity of the transcytosis processes at the BBB, this hurdle is also in great part due to the poor pharmacokinetic (PK) proprieties of highly hydrophilic negatively charged oligonucleotides. These compounds are rapidly removed from circulation after systemic administrations, which limits their delivery to the brain. Thus, strategies that disrupt the BBB and allow fast transfer of compounds from the blood to the brain represent an attractive alternative to enable delivery of conjugated oligonucleotides to the brain upon systemic administrations.

After systemic administrations, DHA-conjugated hsiRNAs have been shown to rapidly associate with serum proteins, such as high-density lipoproteins (HDLs) and albumin.[31] This effect greatly improves circulating times and reduces renal clearance, which may provide a strategic advantage for transvascular brain delivery.[8,31] After BBB disruption, PC-DHA-hsiRNAs accumulated in various regions of the rat brain and were actively internalized by neurons and astrocytes. Similar to what was previously reported after intrastriatal injections,[6,7] in this study the PC-DHA modality played an important role in facilitating tissue accumulation and granting cellular uptake within the CNS. In contrast, unconjugated siRNAs showed poor tissue retention in the brain parenchyma after transvascular delivery to the brain. Detailed studies are now warranted to establish the cellular uptake efficiency of PC-DHA-hsiRNAs in regions of the brain of high delivery (striatum, thalamus, and hippocampus). These studies are required to further our understanding on PK/pharmacodynamic (PD) relationships of conjugated therapeutic oligonucleotides delivered through BBB-disruption approaches.

After transvascular delivery, PC-DHA-hsiRNAs silenced their target mRNA with high specificity and potency, to a similar extent to what was observed in previous dose-response studies in the brain.[6,7] Although transvascular delivery of PC-DHA-hsiRNA reduced *Htt* mRNA in multiple regions of the brain, a significant reduction of HTT protein was detected only in the thalamus, where the highest levels of PC-DHA-hsiRNAs accumulated. Discrepancies between oligonucleotide-mediated silencing of *Htt* mRNA and HTT protein levels have been linked to the slow turnover of HTT protein.[12] For example, Kordasiewicz et al.[12] found that by the end of a 2-week i.c.v. infusion of ASOs, *Htt* mRNA levels were at their lowest, but it took another 2–4 weeks for maximal silencing of HTT protein. Thus, regions of the brain where transvascular delivery of

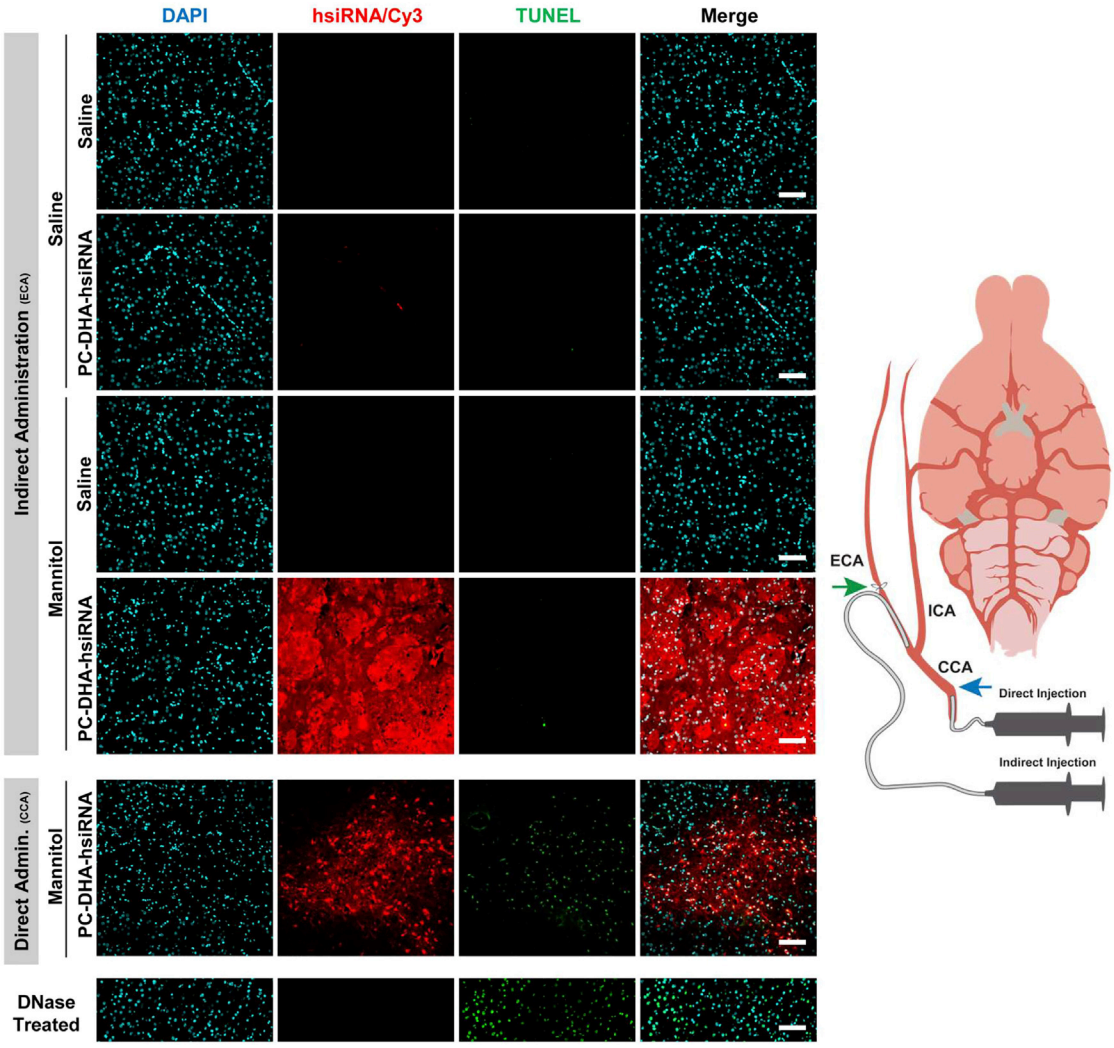

Figure 6. Delivery of PC-DHA-hsiRNA through the External Carotid Artery Limits Apoptosis in the Rat Striatum

Cy3-labeled PC-DHA-hsiRNAs were administered through the right carotid artery preceded by saline or mannitol, and rats were euthanized 48 hr after injections. Schematic to the right illustrates the direct administration (15 mg/kg) carried out through the common carotid artery (CCA) and the indirect injection (37 mg/kg) performed by cannulation of the external carotid artery (ECA). The respective arteries were permanently ligated after administrations at the sites indicated by the blue arrow (CCA) and green arrow (ECA). Fluorescent images (20× objective) of the striatum show PC-DHA-hsiRNA (cy3, red), nuclei (DAPI, cyan), and apoptotic nuclei (TUNEL, green). The DNase-treated sample was used as TUNEL-positive control. n = 2–3 animals/group. Scale bars, 100 μm.

PC-DHA-hsiRNAs significantly reduced *Htt* mRNA levels might also exhibit significant reductions in HTT protein at later time points. Furthermore, follow-up studies aimed at determining the therapeutic utility of this transvascular strategy for Huntington's disease (HD) must include confirmatory dose-response studies, protein assessments at later time points, systematic evaluations of improvements in HD neuropathology (e.g., immunostaining to monitor HTT inclusion formation), and behavior phenotype (e.g., motor coordination, depressive-like behavior, etc.) in appropriate animal models of disease. Although HTT-lowering strategies are currently being evaluated as potential therapeutics for HD,[32,33] we anticipate a more immediate application of this transvascular approach for oligonucleotide delivery in cancer therapeutics. Given the lower risk-benefit ratio in terminal cancers, and the fact that several clinical trials have already been conducted using BBB-disruption strategies for delivery of chemotherapeutics,[15–18] this transvascular gene silencing strategy might find a more rapid translation for the treatment of high-grade malignant brain tumors.

Other strategies to disrupt the BBB have been tested for their ability to enhance transvascular delivery of oligonucleotides to the brain with varying degrees of success. Magnetic resonance imaging-guided focused ultrasound (MRgFUS) causes microbubbles to oscillate within the brain vessels, resulting in shear stress that disrupts the

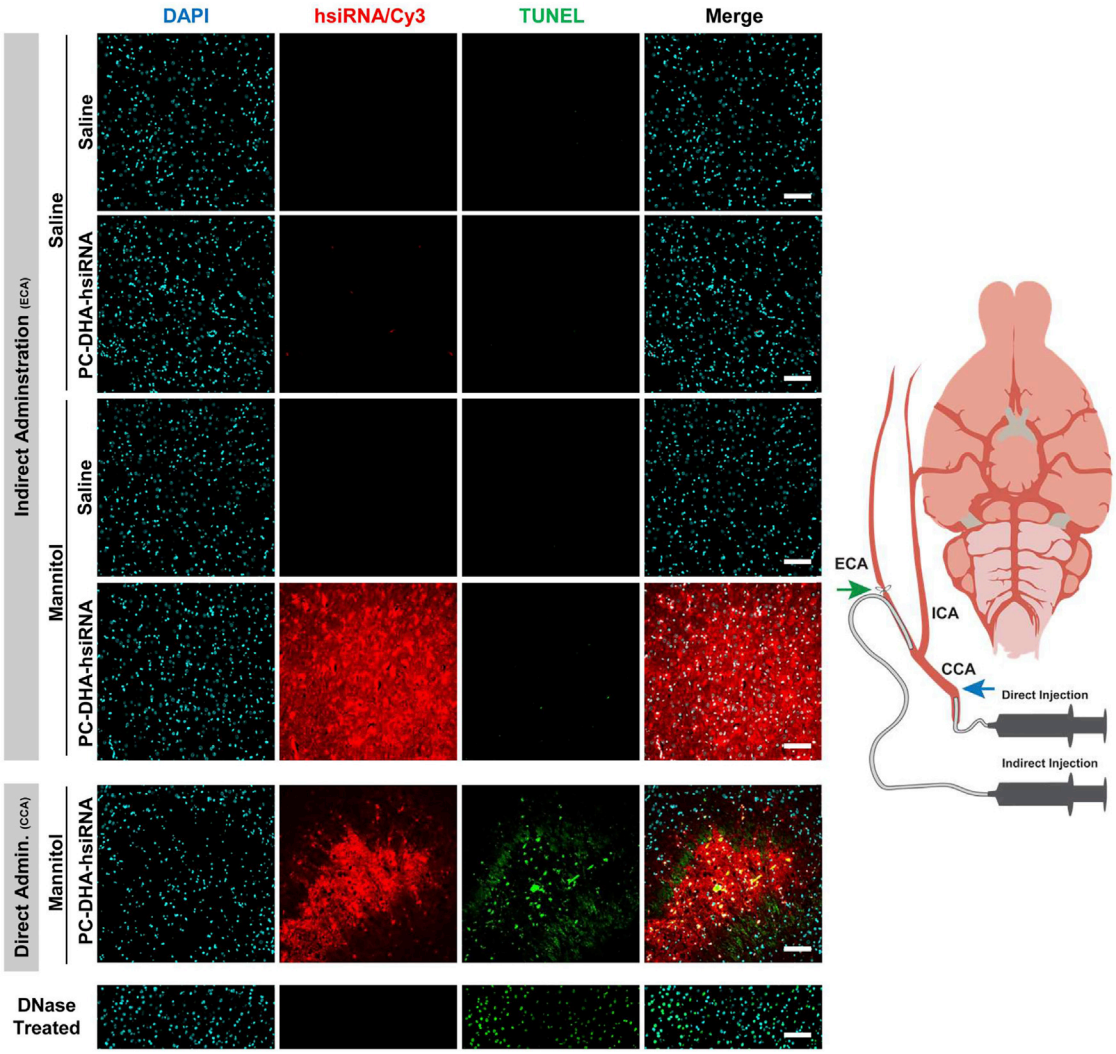

Figure 7. Delivery of PC-DHA-hsiRNA through the External Carotid Artery Limits Apoptosis in the Rat Thalamus

Cy3-labeled PC-DHA-hsiRNAs were administered through the right carotid artery preceded by saline or mannitol, and rats were euthanized 48 hr after injections. Schematic to the right illustrates the direct administration (15 mg/kg) carried out through the common carotid artery (CCA) and the indirect injection (37 mg/kg) performed by cannulation of the external carotid artery (ECA). The respective arteries were permanently ligated after administrations at the sites indicated by the blue arrow (CCA) and green arrow (ECA). Fluorescent images (20× objective) of the thalamus show PC-DHA-hsiRNA (cy3, red), nuclei (DAPI, cyan), and apoptotic nuclei (TUNEL, green). The DNase-treated sample was used as TUNEL-positive control. n = 2–3 animals/group. Scale bars, 100 μm.

tight junctions of the endothelial wall.[34] MRgFUS has been used to improve permeability of the BBB to therapeutic oligonucleotides in focal regions within the brain.[35,36] Using this approach, Burgess et al.[35] delivered cholesterol-conjugated siRNAs to the mouse striatum and induced significant *Htt* mRNA silencing (up to ~32%) within this brain structure. Intracarotid administration of the vasoactive agent, bradykinin, has also been used to increase permeability of the BBB and selectively deliver ASOs to brain tumors.[37,38] Brain tumor vessels that express high levels of B2 receptors and nitric oxide (NO) synthase activity drive oligonucleotide delivery to neoplastic tissue and enable negligible delivery to healthy brain tissue.[38] The utility of these approaches for broad distribution of fully stabilized therapeutic oligonucleotides within the brain remains to be shown.

Transvascular delivery of PC-DHA-hsiRNAs was achieved without causing major neurotoxic effects. DHA-conjugated hsiRNAs have been previously shown to have favorable safety profiles in the brain, maintaining good neuronal integrity and reduced innate immune response compared with Chol-hsiRNAs.[7] In our studies, we detected elevation of GFAP, a marker for astrogliosis, suggesting a mild inflammatory response. Consistent with previous findings for PC-DHA-hsiRNAs,[6] these effects seem to be sequence independent. Although the present transvascular delivery study required doses

substantially higher than what is conventionally used in studies targeting organs such as the liver, no major signs of systemic toxicity were observed in a comprehensive blood chemistry panel. Furthermore, additional systemic toxicological assessments in the lab have shown that PC-DHA-hsiRNAs are well tolerated up to 100 mg/kg and do not induce significant pro-inflammatory cytokine release (A.A. Turanov, A.H.C., and B.M.D.C.G., unpublished data). Together, this further validates PC-DHA-hsiRNAs as a good pre-clinical candidate for both CNS and systemic applications with a wide therapeutic index.

Minimal toxicity within the CNS also depended on the transient nature of mannitol-induced disruption of the BBB, which reportedly reaches maximal permeability within 5–10 min and is then rapidly reestablished.[39–41] Although mannitol is a well-established first-line treatment to reduce intracranial edema after traumatic brain injury,[42,43] little is known about its safety as a BBB-disrupting agent for drug delivery to the brain. In this study, disruption of the BBB did not cause significant cell death or local inflammation in the brain, or cause significant systemic toxicity. Focal ischemic areas were observed only if the CCA was ligated, likely as a result of incomplete cerebral reperfusion and mannitol washout. Neither we nor others observed lasting damage to the BBB,[44] but mannitol-induced seizures and brain edema have been described in cancer patients subjected to BBB disruption for chemotherapy administration.[45] This may assume particular importance when repetitive BBB disruptions are required to ensure sustained mRNA knockdown in the brain. Thus, although current therapeutic oligonucleotide technologies enable gene silencing to endure for months,[1,2,12] further studies are needed to establish the long-term safety of BBB disruption approaches for the delivery of siRNA and ASOs to the brain.

In conclusion, this study provides valuable proof-of-concept for the utility of mannitol-based BBB disruption strategies for productive brain delivery of therapeutic oligonucleotides conjugated to neuroactive ligands. Here we report efficient transvascular delivery of PC-DHA-hsiRNAs after mannitol-mediated disruption of the BBB and potent silencing of *Htt* mRNA in various regions of the rat brain. In this study, PC-DHA was selected as a model ligand because of its advanced features for both systemic and CNS applications; however, we foresee that this approach may be applicable to many other siRNAs conjugated to suitable neuroactive modalities of interest. Furthermore, although *Htt* was used as a model mRNA target, this approach could in principle be applied to treat other genetically defined diseases. Until the long-term effects of repetitive BBB disruptions on brain homeostasis are determined, we envision the approach as a one-time treatment of life-threatening brain tumors. Thus, our findings establish the first successful evidence of the utility of pharmacological-based BBB disruption approaches for meaningful transvascular delivery of therapeutic oligonucleotides to the brain.

MATERIALS AND METHODS

Our manuscript was written according to ARRIVE (Animal Research: Reporting of In Vivo Experiments) guidelines, and experimental protocols involving animals were approved by the University of Massachusetts Medical School Institutional Animal Care and Use Committee (IACUC Protocol #A-2411) and performed according to the guidelines and regulations therein. All experiments were conducted in a blinded and randomized manner.

Synthesis and Preparation of Conjugated Hydrophobic siRNAs

hsiRNAs consist of fully modified antisense (20-nt) and sense (15-nt) strands, which anneal to form a stable asymmetric duplex. The chemical modification pattern used for metabolic stabilization was previously described in Nikan et al.,[6,7] and the relevant *Htt* targeting sequence was previously identified and validated in Alterman et al.[5] PC-DHA was conjugated to the 3′ end of the sense strand, and oligonucleotides were synthesized and purified as previously described.[6] Purified oligonucleotides were collected, desalted by size-exclusion chromatography using a Sephadex G25 column (GE Healthcare Life Sciences, Marlborough, MA, USA), and dried in a SpeedVac. Duplex formation was assessed by gel electrophoresis. Finally, PC-DHA-hsiRNAs were resuspended in sterile 0.9% sodium chloride (NaCl).

Intracarotid Administrations

Male Sprague-Dawley rats (aged 8–12 weeks, weight ~325 g) were housed on a 12-hr light/12-hr dark cycle with *ad libitum* access to food and water. Spontaneously breathing rats were anesthetized using isoflurane (catalog [Cat.] #NDC 66794-013-10; Piramal Healthcare) (5% induction, 2% for surgery, and 1.5% maintenance) carried by room air at a flow rate of 1 L/min. Body temperature was monitored continuously with a rectal probe and maintained at 37.0°C ± 0.5°C with a thermostatically controlled heating lamp. Animals were positioned in a supine position, and a longitudinal incision was made at the level of the neck to expose the carotid artery. After isolation and permanent ligation of the occipital artery and pterygopalatine arteries, a PE-10 catheter was retrogradely inserted into the ECA and advanced to the level of the bifurcation of the CCA. The distal end of the ECA was then ligated and cut to allow ~180° rotation of the ECA stump containing the PE-10 catheter. This approach facilitated the alignment with the proximal end of the internal carotid artery (ICA) branch for delivery of solutions. Sterile 25% mannitol (Cat. #NDC 0409-4031-01; Hospira) or saline (0.9% NaCl, Cat. #NDC 0409-4888-02; Hospira) was injected at a rate of 0.09 mL/s for 25 s, as described in Martin et al.[46] After 5 min, ~600 μL of PC-DHA-hsiRNA was injected over 25 s. For biodistribution studies, a final dose of 37 mg/kg PC-DHA-hsiRNA was administered, whereas for gene silencing efficacy studies a final dose of 16 mg/kg was used. ~200 μL of saline was used to flush the dead volume of the catheter immediately after each injection. During injections, the CCA was transiently clamped using an aneurysm clip and released after each injection to allow circulation of blood. Following all injections, the proximal end of the ECA was ligated, the PE-10 catheter removed, and wounds closed. To alleviate pain and discomfort, animals received carprofen (5 mg/kg) (NADA #141-199; Rimadyl [Pfizer]), administered subcutaneously. HydroGel and food pellets were placed at the floor of the cage to facilitate hydration and nutrition.

Biodistribution Studies

For biodistribution studies, animals were euthanized 48 hr post-injections and perfused with PBS (diluted from 10× PBS, Cat. #BM-221; Boston Bioproducts) for 15 min at 5 mL/min. Brains were removed and sliced using a brain matrix.

Fluorescent Imaging

Tissues for imaging were post-fixed overnight in 10% formalin at 4°C, embedded in paraffin, cut into 4-μm sections, and mounted on slides for staining. Subsequently, sections were deparaffinized by two rounds of incubation in xylene (8 min) and rehydrated in a series of ethanol dilutions (100%, 95%, and 80%, 4 min each). Slides were washed in PBS for 2 min. For NeuN and GFAP immunostaining, antigen retrieval was achieved by boiling sections for 5 min in 10 mM Tris, 1 mM EDTA (pH 9.0). Sections were cooled to room temperature for 20 min. Sections were soaked in PBS for 5 min and blocked with 5% normal goat serum in PBS containing 0.05% Tween 20 (PBST) (Tween 20, Cat. #BP337-100; Fisher Bioreagents). Slides were washed for 5 min with PBST and incubated for 1 hr with the primary antibodies: mouse anti-mouse NeuN (1:1,000; Cat. #MAB377; Millipore) and rabbit anti-mouse GFAP (1:340; Cat. #Z0334; Dako). Sections were washed for 5 min with PBST and then incubated for 30 min with secondary antibodies: Alexa Fluor 488-labeled anti-mouse IgG (1:1,000; Cat. #A11001; Life Technologies) or DyLight 649-labeled anti-rabbit IgG (1:1,000; Cat. #ab96902; Abcam). Tissues were washed three times for 5 min with PBST and stained with DAPI for 2 min. PermaFluor mounting medium (Cat. #TA-030-FM; Thermo Scientific) was used to place glass coverslips, and slides were left to dry at 4°C overnight protected from light.

Leica DMi8 fluorescent microscope fitted with a Hamamatsu C11440 ORCA-Flash 4.0 was used to acquire tiled-arrays of brain coronal sections (20× objective) and high-resolution images (63× objective). Images within the same panel were acquired under the same light intensity settings and exposure times set individually for each channel. The quick look-up table (LUT) tool and intensity histograms were used to ensure that images were acquired within the dynamic range of the detector and without significant pixel saturation.

Peptide Nucleic Acid Hybridization Assay

In each treatment group, two to three animals were dedicated for biodistribution studies, in which hsiRNA guide strands in tissue lysates were quantified using a PNA-based hybridization assay. Various regions of the brain were dissected from PBS-perfused animals, and ~30 mg of tissue was suspended in 300 μL lysis solution (Cat. #MTC096H; MasterPure; Epicentre) containing ~0.2 mg/mL Proteinase K (Cat. #25530-049; Invitrogen) and lysed in a QIAGEN TissueLyser II for 60 min at 55°C. SDS was precipitated by adding 20 μL of 3 M potassium chloride and pelleted by centrifugation for 15 min at 4,000 × *g*. Clear supernatants were diluted with 150 μL of hybridization buffer (50 mM Tris, 10% acetonitrile [ACN], pH 8.8) containing 5 pmol of HTT Cy3-labeled PNA (PNABio, Thousand Oaks, CA, USA). Samples were heated for 15 min at 95°C and annealed for 15 min at 55°C on a Bio-Rad c1000 thermal cycler. Samples were cooled to room temperature and then frozen and stored at −80°C until analysis. Samples were analyzed by chromatography through a DNAPac PA100 anion exchange column (Cat. #043010; Thermo Fisher Scientific) using a buffer gradient. Mobile phase buffers consisted of buffer A (50% water; 50% ACN; 25 mM Tris-HCl [pH 8.5]; 1 mM EDTA) and buffer B (800 mM $NaClO_4$ in buffer A). Cy3-PNA-guide strand hybrids were eluted within 2.5 min using a steep gradient from 10% to 100% buffer B. Fluorescent peaks (550 nm excitation/570 nm emission) were monitored and integrated. Samples were calibrated by analyzing tissue samples spiked with known amounts of hsiRNA duplex. Final guide strand concentrations were calculated by correlating the area under the curve (AUC) obtained for each sample against the standards.

Gene Silencing Efficacy Studies

For gene silencing assays, animals were euthanized 7 days after intracarotid administration of PC-DHA-hsiRNA (16 mg/kg). Coronal sections (300 μm) were prepared using a Leica Vibratome vt1000s. Three alternate sections were used for mRNA quantification or protein assessment, and 2-mm tissue punch biopsies were taken from the injected side. Alternatively, 1.5-mm punches were taken from structures such as the hippocampus, thalamus, cerebellum, and brainstem from regions dissected manually. Biopsies for mRNA assessment were incubated overnight at 4°C in RNAlater (Cat. #R0901; Sigma-Aldrich) and stored at −80°C. Biopsies for western blot analyses were flash frozen in liquid nitrogen and stored at −80°C.

mRNA Quantification

For mRNA quantification, tissue punches were lysed for 60 min at 55°C in 300 μL of QuantiGene (QG) homogenizing solution containing ~0.2 mg/mL Proteinase K (#25530-049; Invitrogen) using a Qiagen TissueLyser II. mRNAs were quantified using the Quantigene 2.0 branched-DNA (b-DNA) assay (Affymetrix) as described.[47] In brief, 60 μL of rat *Htt* (Cat. #SC-34753; Affymetrix) or *Ppib* (Cat. #SC-10013; Affymetrix) probe sets were placed on a QuantiGene b-DNA capture plate followed by 40 μL of diluted or undiluted tissue lysate. Plates were sealed with film and incubated overnight. Signal was amplified using the manufacturer's protocol, and luminescence was measured on a Tecan Infinite M1000 microplate reader. Relative gene silencing was calculated by normalizing the level of *Htt* mRNA to that of the housekeeping gene *Ppib* in all samples and displayed as percentage of saline control; n = 7 or 8 per group.

Western Blots

Tissue punches from different regions of brain were homogenized on ice in 10 mM HEPES (pH 7.2), 250 mM sucrose, 1 mM EDTA containing protease inhibitor tablets (complete, mini, EDTA-free; Cat. #11836170001; Roche) and sonicated for 10 s. Protein concentration was determined using the Bradford method (Cat. #500-0006; Bio-Rad). Protein lysates (10 μg) were loaded on a SDS-polyacrylamide 3%–8% Tris-acetate gels (Cat. #EA03875BOX; Life Technologies) and separated for 90 min at 120 V. Proteins were transferred to

nitrocellulose membranes using the Bio-Rad TransBlot Turbo transfer system. Membranes were blocked for 1 hr at room temperature with 5% non-fat milk in TBST-0.1%. Membranes were washed with TBST-0.1% and incubated with primary antibodies against HTT (Ab1[48]) and GFAP (Cat. #AB5804; EMD Millipore) overnight at 4°C. Membranes were washed with TBST-0.1% and incubated with the horseradish peroxidase-conjugated anti-rabbit and anti-mouse IgG antibodies (Cat. #711-035-152 and 715-035-150; Jackson Immunoresearch) for 1 hr at room temperature. Proteins were detected by incubating membranes with SuperSignal West Pico Chemiluminescent Substrate (Cat. #34080; Thermo Scientific) and exposing the membrane to Hyperfilm ECL (Cat. #28906839; GE Healthcare). Membranes were imaged using a CCD imaging system (Alpha Innotech) or Epson Perfection V750 Pro scanner. Membranes were re-probed to detect β-actin as a housekeeping control (Cat. #A5441; Sigma-Aldrich). Densitometry analysis was performed using ImageJ; HTT and GFAP levels were normalized to β-actin levels, and results were expressed relative to saline control; n = 7–8 rats per group.

Statistical Analysis

Unless otherwise stated, continuous variables are reported as mean ± SD. Normality of data was examined using Shapiro-Wilk test. Between-group comparisons for continuous variables were made by one-way ANOVA with Tukey's post hoc test. Two-sided significance tests were used throughout, and a two-sided $p < 0.05$ was considered statistically significant. All statistical analyses were performed using GraphPad Prism 7.

SUPPLEMENTAL INFORMATION

Supplemental Information includes Supplemental Materials and Methods and six figures and can be found with this article online at https://doi.org/10.1016/j.ymthe.2018.08.005.

AUTHOR CONTRIBUTIONS

N.H., A.K., and N.A. supervised experimental design and assisted with manuscript editing. J.B. performed all *in vivo* intracarotid administrations. J.F.A., J.W.G., and A.H.C. assisted with sample collection, processing, and analysis. A.B., M.N., and D.E. synthesized and purified hsiRNA conjugates. E.S. and M.D. contributed with western blot assays and respective analyses. B.M.D.C.G. designed and executed experiments, critically analyzed data, and wrote the manuscript.

CONFLICTS OF INTEREST

A.K. owns stock at RXi Pharmaceuticals and Advirna LLC, which holds a patent on asymmetric, hydrophobically modified siRNAs. N.H. serves on the advisory board of Omniox, Inc. The remaining authors do not have any competing financial interest to disclose.

ACKNOWLEDGMENTS

This work was supported by the CHDI Foundation (research agreement A-6119 and JSC A6367) and the NIH (grants RO1GM10880302, RO1NS03819415, UH3TR00088803, and S10OD020012). B.M.D.C.G. was supported by a Milton-Safenowitz Fellowship (grant 17-PDF-363) from the Amyotrophic Lateral Sclerosis Association (ALSA). N.H. was supported by grant K08NS091499 from the National Institute of Neurological Disorders and Stroke of the NIH. The authors acknowledge Dr. Darryl Conte, Jr. for editorial feedback on the manuscript and Dr. Maire Osborn for the oligonucleotide PyMOL molecular structure in Figure 1. The content is solely the responsibility of the authors and does not necessarily represent the official views of the NIH.

REFERENCES

1. Haraszti, R.A., Roux, L., Coles, A.H., Turanov, A.A., Alterman, J.F., Echeverria, D., Godinho, B.M.D.C., Aronin, N., and Khvorova, A. (2017). 5′-Vinylphosphonate improves tissue accumulation and efficacy of conjugated siRNAs in vivo. Nucleic Acids Res. *45*, 7581–7592.

2. Hassler, M.R., Turanov, A.A., Alterman, J.F., Haraszti, R.A., Coles, A.H., Osborn, M.F., Echeverria, D., Nikan, M., Salomon, W.E., Roux, L., et al. (2018). Comparison of partially and fully chemically-modified siRNA in conjugate-mediated delivery in vivo. Nucleic Acids Res. *46*, 2185–2196.

3. Pasi, K.J., Rangarajan, S., Georgiev, P., Mant, T., Creagh, M.D., Lissitchkov, T., Bevan, D., Austin, S., Hay, C.R., Hegemann, I., et al. (2017). Targeting of antithrombin in hemophilia A or B with RNAi therapy. N. Engl. J. Med. *377*, 819–828.

4. Ray, K.K., Landmesser, U., Leiter, L.A., Kallend, D., Dufour, R., Karakas, M., Hall, T., Troquay, R.P., Turner, T., Visseren, F.L., et al. (2017). Inclisiran in patients at high cardiovascular risk with elevated LDL cholesterol. N. Engl. J. Med. *376*, 1430–1440.

5. Alterman, J.F., Hall, L.M., Coles, A.H., Hassler, M.R., Didiot, M.-C., Chase, K., Abraham, J., Sottosanti, E., Johnson, E., Sapp, E., et al. (2015). Hydrophobically modified siRNAs silence Huntingtin mRNA in primary neurons and mouse brain. Mol. Ther. Nucleic Acids *4*, e266.

6. Nikan, M., Osborn, M.F., Coles, A.H., Biscans, A., Godinho, B.M.D.C., Haraszti, R.A., Sapp, E., Echeverria, D., DiFiglia, M., Aronin, N., and Khvorova, A. (2017). Synthesis and evaluation of parenchymal retention and efficacy of a metabolically stable O-phosphocholine-N-docosahexaenoyl-l-serine siRNA conjugate in mouse brain. Bioconjug. Chem. *28*, 1758–1766.

7. Nikan, M., Osborn, M.F., Coles, A.H., Godinho, B.M., Hall, L.M., Haraszti, R.A., Hassler, M.R., Echeverria, D., Aronin, N., and Khvorova, A. (2016). Docosahexaenoic acid conjugation enhances distribution and safety of siRNA upon local administration in mouse brain. Mol. Ther. Nucleic Acids *5*, e344.

8. Godinho, B.M.D.C., Gilbert, J.W., Haraszti, R.A., Coles, A.H., Biscans, A., Roux, L., Nikan, M., Echeverria, D., Hassler, M., and Khvorova, A. (2017). Pharmacokinetic profiling of conjugated therapeutic oligonucleotides: a high-throughput method based upon serial blood microsampling coupled to peptide nucleic acid Hybridization assay. Nucleic Acid Ther. *27*, 323–334.

9. Boursereau, R., Donadieu, A., Dabertrand, F., Dubayle, D., and Morel, J.-L. (2015). Blood brain barrier precludes the cerebral arteries to intravenously-injected antisense oligonucleotide. Eur. J. Pharmacol. *747*, 141–149.

10. Kuwahara, H., Nishina, K., Yoshida, K., Nishina, T., Yamamoto, M., Saito, Y., Piao, W., Yoshida, M., Mizusawa, H., and Yokota, T. (2011). Efficient in vivo delivery of siRNA into brain capillary endothelial cells along with endogenous lipoprotein. Mol. Ther. *19*, 2213–2221.

11. Finkel, R.S., Mercuri, E., Darras, B.T., Connolly, A.M., Kuntz, N.L., Kirschner, J., Chiriboga, C.A., Saito, K., Servais, L., Tizzano, E., et al.; ENDEAR Study Group (2017). Nusinersen versus sham control in infantile-onset spinal muscular atrophy. N. Engl. J. Med. *377*, 1723–1732.

12. Kordasiewicz, H.B., Stanek, L.M., Wancewicz, E.V., Mazur, C., McAlonis, M.M., Pytel, K.A., Artates, J.W., Weiss, A., Cheng, S.H., Shihabuddin, L.S., et al. (2012). Sustained therapeutic reversal of Huntington's disease by transient repression of huntingtin synthesis. Neuron *74*, 1031–1044.

13. Rigo, F., Chun, S.J., Norris, D.A., Hung, G., Lee, S., Matson, J., Fey, R.A., Gaus, H., Hua, Y., Grundy, J.S., et al. (2014). Pharmacology of a central nervous system delivered 2′-O-methoxyethyl-modified survival of motor neuron splicing oligonucleotide in mice and nonhuman primates. J. Pharmacol. Exp. Ther. *350*, 46–55.

14. Hersh, D.S., Wadajkar, A.S., Roberts, N., Perez, J.G., Connolly, N.P., Frenkel, V., Winkles, J.A., Woodworth, G.F., and Kim, A.J. (2016). Evolving drug delivery strategies to overcome the blood brain barrier. Curr. Pharm. Des. *22*, 1177–1193.

15. Guillaume, D.J., Doolittle, N.D., Gahramanov, S., Hedrick, N.A., Delashaw, J.B., and Neuwelt, E.A. (2010). Intra-arterial chemotherapy with osmotic blood-brain barrier disruption for aggressive oligodendroglial tumors: results of a phase I study. Neurosurgery *66*, 48–58, discussion 58.

16. Boockvar, J.A., Tsiouris, A.J., Hofstetter, C.P., Kovanlikaya, I., Fralin, S., Kesavabhotla, K., Seedial, S.M., Pannullo, S.C., Schwartz, T.H., Stieg, P., et al. (2011). Safety and maximum tolerated dose of superselective intraarterial cerebral infusion of bevacizumab after osmotic blood-brain barrier disruption for recurrent malignant glioma. Clinical article. J. Neurosurg. *114*, 624–632.

17. Burkhardt, J.-K., Riina, H., Shin, B.J., Christos, P., Kesavabhotla, K., Hofstetter, C.P., Tsiouris, A.J., and Boockvar, J.A. (2012). Intra-arterial delivery of bevacizumab after blood-brain barrier disruption for the treatment of recurrent glioblastoma: progression-free survival and overall survival. World Neurosurg. *77*, 130–134.

18. Chakraborty, S., Filippi, C.G., Wong, T., Ray, A., Fralin, S., Tsiouris, A.J., Praminick, B., Demopoulos, A., McCrea, H.J., Bodhinayake, I., et al. (2016). Superselective intra-arterial cerebral infusion of cetuximab after osmotic blood/brain barrier disruption for recurrent malignant glioma: phase I study. J. Neurooncol. *128*, 405–415.

19. McCarty, D.M., DiRosario, J., Gulaid, K., Muenzer, J., and Fu, H. (2009). Mannitol-facilitated CNS entry of rAAV2 vector significantly delayed the neurological disease progression in MPS IIIB mice. Gene Ther. *16*, 1340–1352.

20. Fu, H., Muenzer, J., Samulski, R.J., Breese, G., Sifford, J., Zeng, X., and McCarty, D.M. (2003). Self-complementary adeno-associated virus serotype 2 vector: global distribution and broad dispersion of AAV-mediated transgene expression in mouse brain. Mol. Ther. *8*, 911–917.

21. Foley, C.P., Rubin, D.G., Santillan, A., Sondhi, D., Dyke, J.P., Crystal, R.G., Gobin, Y.P., and Ballon, D.J. (2014). Intra-arterial delivery of AAV vectors to the mouse brain after mannitol mediated blood brain barrier disruption. J. Control. Release *196*, 71–78.

22. Muldoon, L.L., Nilaver, G., Kroll, R.A., Pagel, M.A., Breakefield, X.O., Chiocca, E.A., Davidson, B.L., Weissleder, R., and Neuwelt, E.A. (1995). Comparison of intracerebral inoculation and osmotic blood-brain barrier disruption for delivery of adenovirus, herpesvirus, and iron oxide particles to normal rat brain. Am. J. Pathol. *147*, 1840–1851.

23. Jiao, S., Miller, P.J., and Lapchak, P.A. (1996). Enhanced delivery of [125I]glial cell line-derived neurotrophic factor to the rat CNS following osmotic blood-brain barrier modification. Neurosci. Lett. *220*, 187–190.

24. Banks, W.A., Farr, S.A., Butt, W., Kumar, V.B., Franko, M.W., and Morley, J.E. (2001). Delivery across the blood-brain barrier of antisense directed against amyloid β: reversal of learning and memory deficits in mice overexpressing amyloid precursor protein. J. Pharmacol. Exp. Ther. *297*, 1113–1121.

25. Chen, K.-B., Wei, V.C., Yen, L.F., Poon, K.-S., Liu, Y.-C., Cheng, K.-S., Chang, C.S., and Lai, T.W. (2013). Intravenous mannitol does not increase blood-brain barrier permeability to inert dyes in the adult rat forebrain. Neuroreport *24*, 303–307.

26. Sakamoto, A., and Ido, T. (1993). Liposome targeting to rat brain: effect of osmotic opening of the blood-brain barrier. Brain Res. *629*, 171–175.

27. Nguyen, L.N., Ma, D., Shui, G., Wong, P., Cazenave-Gassiot, A., Zhang, X., Wenk, M.R., Goh, E.L., and Silver, D.L. (2014). Mfsd2a is a transporter for the essential omega-3 fatty acid docosahexaenoic acid. Nature *509*, 503–506.

28. Ben-Zvi, A., Lacoste, B., Kur, E., Andreone, B.J., Mayshar, Y., Yan, H., and Gu, C. (2014). Mfsd2a is critical for the formation and function of the blood-brain barrier. Nature *509*, 507–511.

29. Zimmermann, T.S., Karsten, V., Chan, A., Chiesa, J., Boyce, M., Bettencourt, B.R., Hutabarat, R., Nochur, S., Vaishnaw, A., and Gollob, J. (2017). Clinical proof of concept for a novel hepatocyte-targeting GalNAc-siRNA conjugate. Mol. Ther. *25*, 71–78.

30. Mäger, I., Meyer, A.H., Li, J., Lenter, M., Hildebrandt, T., Leparc, G., and Wood, M.J.A. (2017). Targeting blood-brain-barrier transcytosis - perspectives for drug delivery. Neuropharmacology *120*, 4–7.

31. Osborn, M.F., Coles, A.H., Biscans, A., Haraszti, R.A., Roux, L., Davis, S., Ly, S., Echeverria, D., Hassler, M.R., Godinho, B.M.D.C., et al. (2018). Hydrophobicity drives the systemic distribution of lipid-conjugated siRNAs via lipid transport pathways. bioRxiv. https://doi.org/10.1101/288092.

32. Godinho, B.M., Malhotra, M., O'Driscoll, C.M., and Cryan, J.F. (2015). Delivering a disease-modifying treatment for Huntington's disease. Drug Discov. Today *20*, 50–64.

33. Rodrigues, F.B., and Wild, E.J. (2018). Huntington's Disease Clinical Trials Corner: February 2018. J. Huntingtons Dis. *7*, 89–98.

34. Aryal, M., Arvanitis, C.D., Alexander, P.M., and McDannold, N. (2014). Ultrasound-mediated blood-brain barrier disruption for targeted drug delivery in the central nervous system. Adv. Drug Deliv. Rev. *72*, 94–109.

35. Burgess, A., Huang, Y., Querbes, W., Sah, D.W., and Hynynen, K. (2012). Focused ultrasound for targeted delivery of siRNA and efficient knockdown of Htt expression. J. Control. Release *163*, 125–129.

36. Rychak, J.J., and Klibanov, A.L. (2014). Nucleic acid delivery with microbubbles and ultrasound. Adv. Drug Deliv. Rev. *72*, 82–93.

37. Bartus, R.T., Elliott, P.J., Dean, R.L., Hayward, N.J., Nagle, T.L., Huff, M.R., Snodgrass, P.A., and Blunt, D.G. (1996). Controlled modulation of BBB permeability using the bradykinin agonist, RMP-7. Exp. Neurol. *142*, 14–28.

38. Koga, H., Inamura, T., Ikezaki, K., Samoto, K., Matsukado, K., and Fukui, M. (1999). Selective transvascular delivery of oligodeoxynucleotides to experimental brain tumors. J. Neurooncol. *43*, 143–151.

39. Cosolo, W.C., Martinello, P., Louis, W.J., and Christophidis, N. (1989). Blood-brain barrier disruption using mannitol: time course and electron microscopy studies. Am. J. Physiol. *256*, R443–R447.

40. Ikeda, M., Bhattacharjee, A.K., Kondoh, T., Nagashima, T., and Tamaki, N. (2002). Synergistic effect of cold mannitol and Na(+)/Ca(2+) exchange blocker on blood-brain barrier opening. Biochem. Biophys. Res. Commun. *291*, 669–674.

41. Rapoport, S.I., Fredericks, W.R., Ohno, K., and Pettigrew, K.D. (1980). Quantitative aspects of reversible osmotic opening of the blood-brain barrier. Am. J. Physiol. *238*, R421–R431.

42. Bratton, S.L., Chestnut, R.M., Ghajar, J., McConnell Hammond, F.F., Harris, O.A., Hartl, R., Manley, G.T., Nemecek, A., Newell, D.W., Rosenthal, G., et al.; Brain Trauma Foundation; American Association of Neurological Surgeons; Congress of Neurological Surgeons; Joint Section on Neurotrauma and Critical Care, AANS/CNS (2007). Guidelines for the management of severe traumatic brain injury. II. Hyperosmolar therapy. J. Neurotrauma *24* (*Suppl 1*), S14–S20.

43. Maas, A.I., Dearden, M., Teasdale, G.M., Braakman, R., Cohadon, F., Iannotti, F., Karimi, A., Lapierre, F., Murray, G., Ohman, J., et al.; European Brain Injury Consortium (1997). EBIC-guidelines for management of severe head injury in adults. Acta Neurochir. (Wien) *139*, 286–294.

44. Wilson, A.J., Evill, C.A., and Sage, M.R. (1991). Effects of nonionic contrast media on the blood-brain barrier. Osmolality versus chemotoxicity. Invest. Radiol. *26*, 1091–1094.

45. Marchi, N., Angelov, L., Masaryk, T., Fazio, V., Granata, T., Hernandez, N., Hallene, K., Diglaw, T., Franic, L., Najm, I., and Janigro, D. (2007). Seizure-promoting effect of blood-brain barrier disruption. Epilepsia *48*, 732–742.

46. Martin, J.A., Maris, A.S., Ehtesham, M., and Singer, R.J. (2012). Rat model of blood-brain barrier disruption to allow targeted neurovascular therapeutics. J. Vis. Exp. (69), e50019.

47. Coles, A.H., Osborn, M.F., Alterman, J.F., Turanov, A.A., Godinho, B.M., Kennington, L., Chase, K., Aronin, N., and Khvorova, A. (2016). A high-throughput method for direct detection of therapeutic oligonucleotide-induced gene silencing in vivo. Nucleic Acid Ther. *26*, 86–92.

48. DiFiglia, M., Sapp, E., Chase, K., Schwarz, C., Meloni, A., Young, C., Martin, E., Vonsattel, J.P., Carraway, R., Reeves, S.A., et al. (1995). Huntingtin is a cytoplasmic protein associated with vesicles in human and rat brain neurons. Neuron. *14*, 1075–1081.

YMTHE, Volume *26*

Supplemental Information

Transvascular Delivery of Hydrophobically Modified siRNAs: Gene Silencing in the Rat Brain upon Disruption of the Blood-Brain Barrier

Bruno M.D.C. Godinho, Nils Henninger, James Bouley, Julia F. Alterman, Reka A. Haraszti, James W. Gilbert, Ellen Sapp, Andrew H. Coles, Annabelle Biscans, Mehran Nikan, Dimas Echeverria, Marian DiFiglia, Neil Aronin, and Anastasia Khvorova

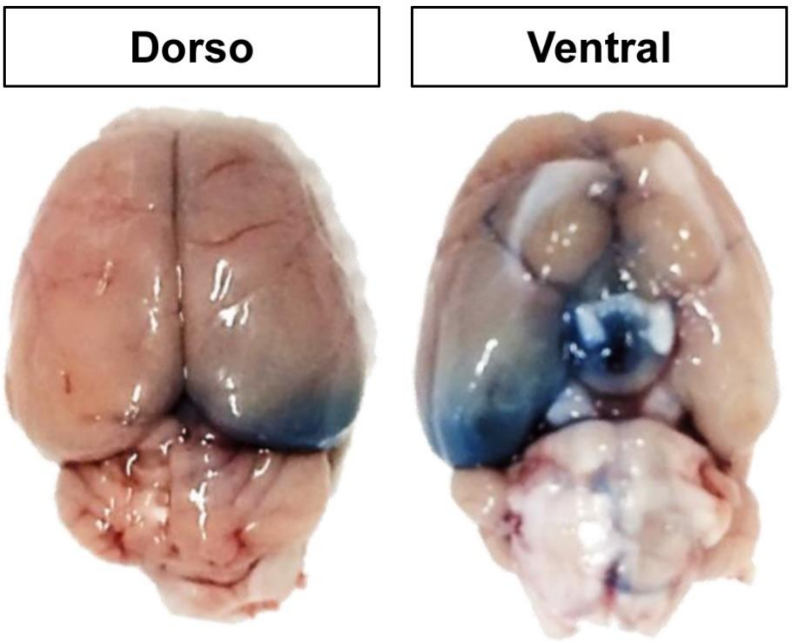

Figure S1. Single intracarotid administration of 25% Mannitol improves brain permeability to Evans blue dye.

Sprague-Dawley male rats ~9 weeks old were treated through the right carotid artery with a single dose of 25% mannitol (2.25 mL) followed by injection of 2% Evans blue dye (600 µL). Animals were euthanized after 48 hours. n = 2 animals.

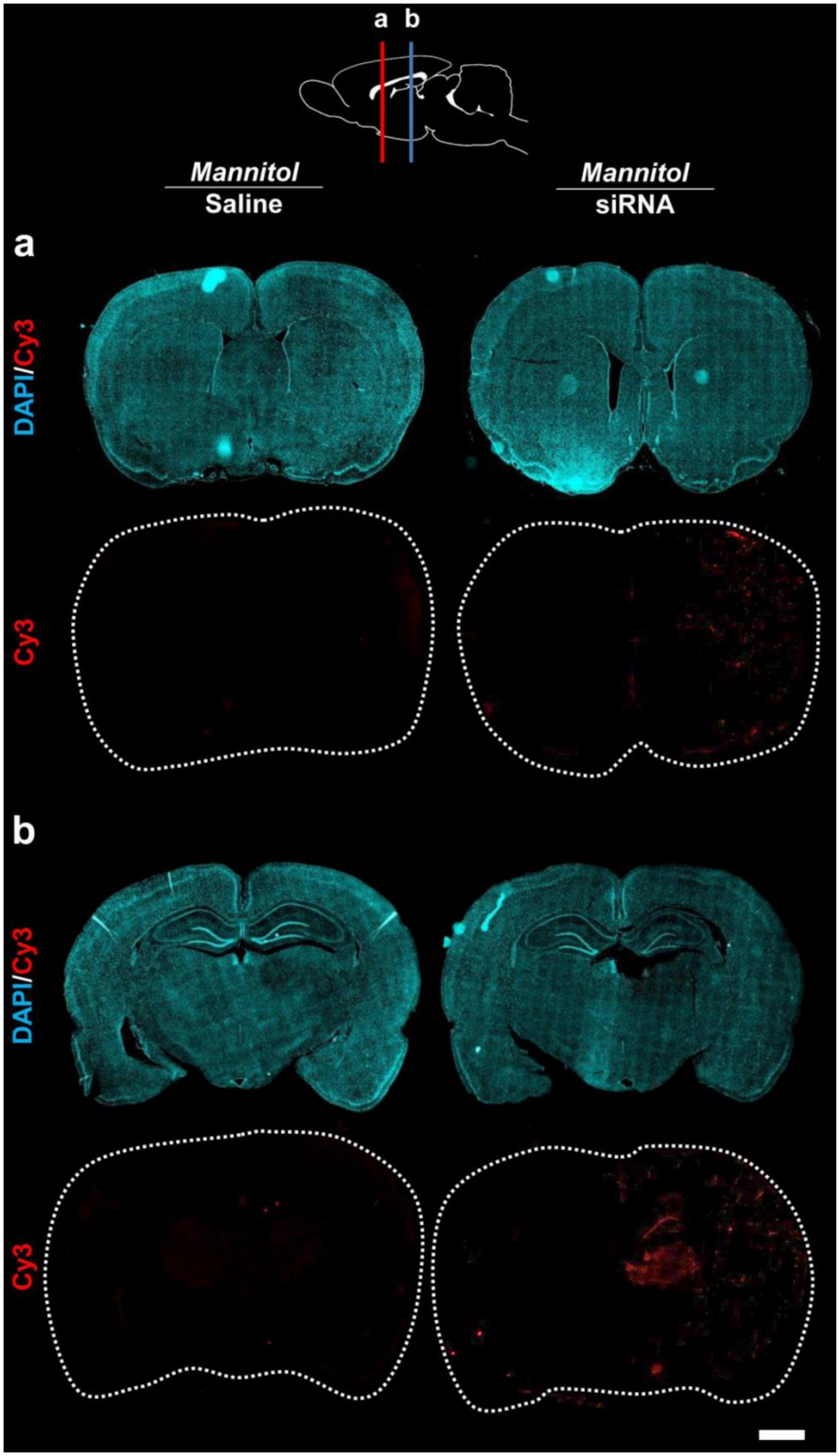

Figure S2. Unconjugated siRNAs present limited retention in the rat brain after transvascular delivery.

Cy3-labelled siRNAs 37 mg/kg were injected through the right carotid artery preceded by mannitol. Animals were euthanized 48 hours after injections and fluorescent tiled arrays obtained from coronal sections (20x objective). The schematic at the top shows the approximate positions of the (a) anterior (red line) and (b) posterior (blue line) sections. Nuclei (DAPI, cyan), Cy3-labelled siRNA (red). Scale bar = 2 mm. n = 2-3 animals/group.

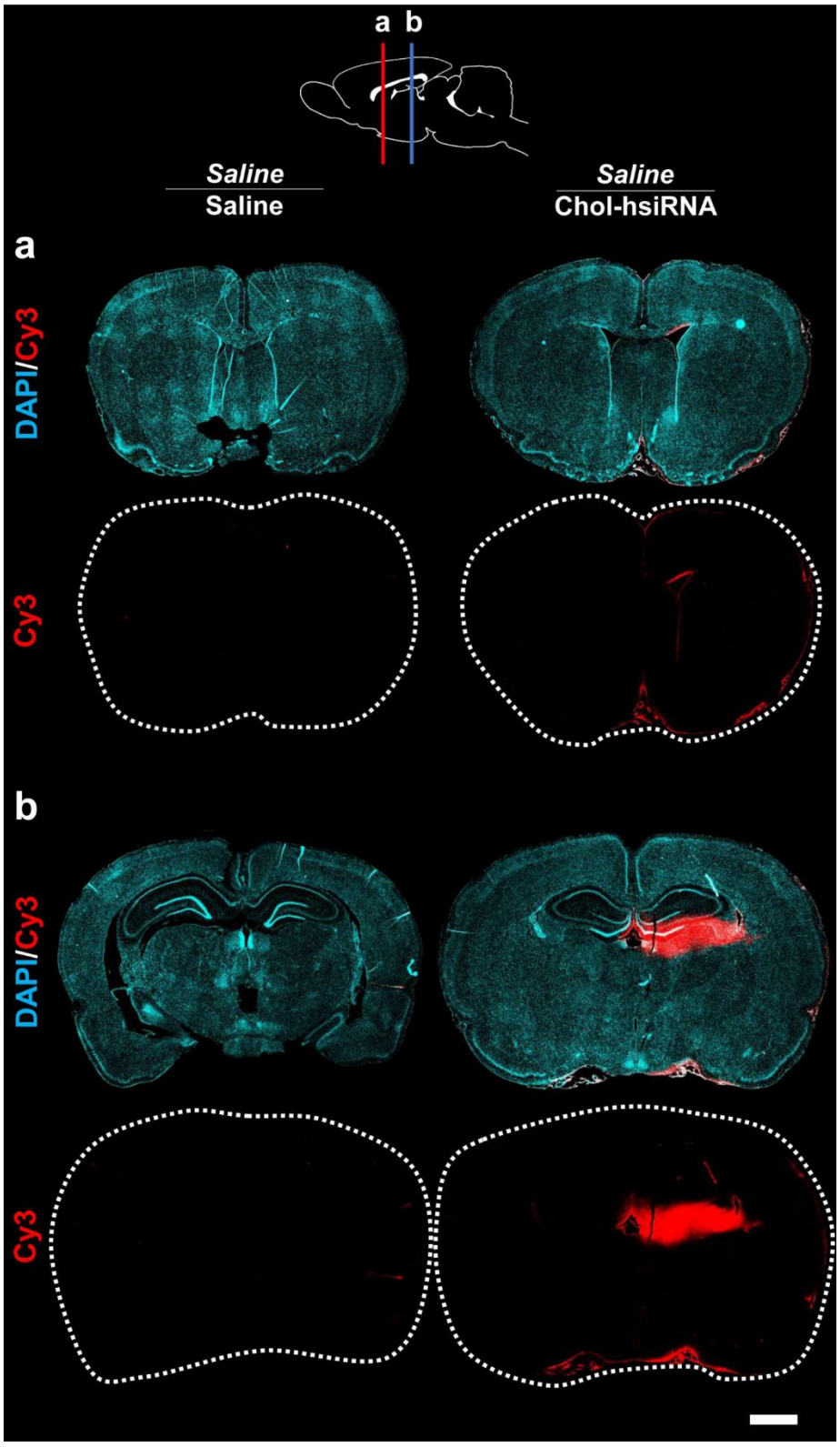

Figure S3. Cholesterol-hsiRNAs present limited transvascular delivery to the rat brain after intracarotid administrations.

Cy3-labelled Cholesterol-conjugated hsiRNAs (Chol-hsiRNAs) 33 mg/kg were injected through the right carotid artery preceded by saline. Animals were euthanized 48 hours after injections and fluorescent tiled arrays obtained from coronal sections (20x objective). The schematic at the top shows the approximate positions of the (a) anterior (red line) and (b) posterior (blue line) sections. Nuclei (DAPI, cyan), Cy3-labelled PC-DHA-hsiRNA (red). Scale bar = 2 mm. n = 2-3 animals/group.

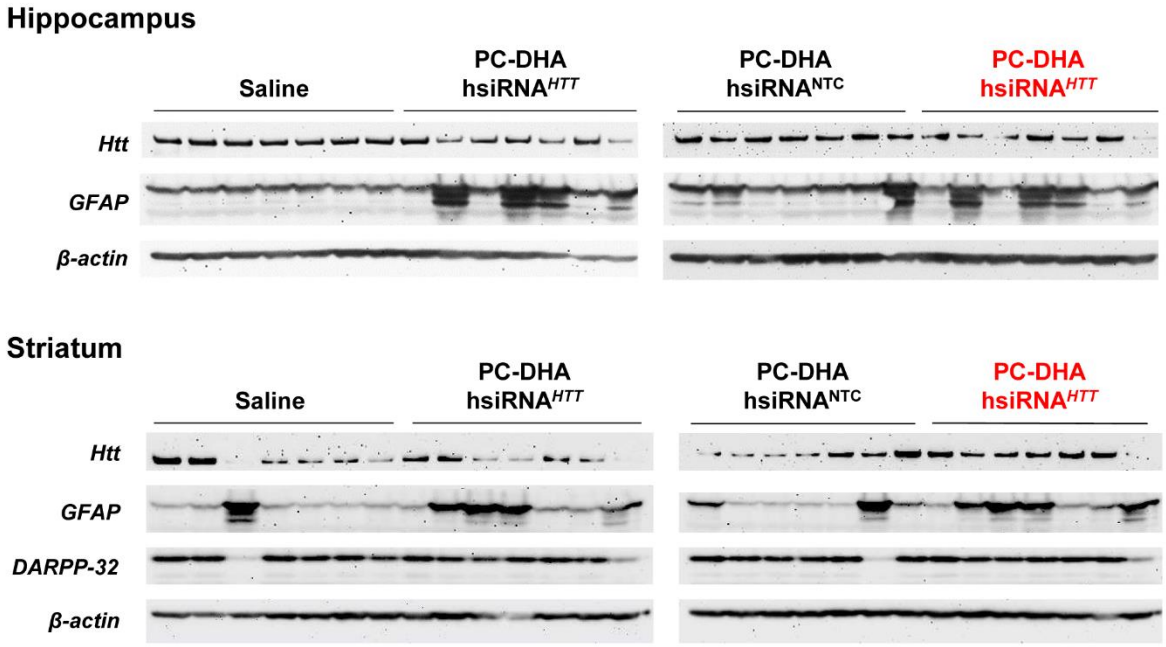

Figure S4. PC-DHA-hsiRNAs present differential reductions on target protein levels in the rat hippocampus and striatum after mannitol-induced blood-brain barrier disruption

PC-DHA-hsiRNAs (16 mg/kg) or saline were administered through the right carotid artery after pre-treatment with mannitol. Huntingtin (HTT)-targeting (PC-DHA-hsiRNA^{HTT}) and non-targeting control (PC-DHA-hsiRNA^{NTC}) sequences were used. HTT, Glial fibrillary acidic protein (GFAP) and Dopamine- and cAMP-regulated phosphoprotein (DARPP-32) expression levels were assessed by western blot 7 days post-injection. Blots depict protein levels from tissue biopsies collected from the dentate gyrus (hippocampus) and caudate putamen (striatum) of the injected side. PC-DHA-hsiRNA^{HTT} samples (red) were analyzed twice in two separate western blots: once with saline (left) and once with PC-DHA-hsiRNA^{NTC} controls. n=7-8 animals/group.

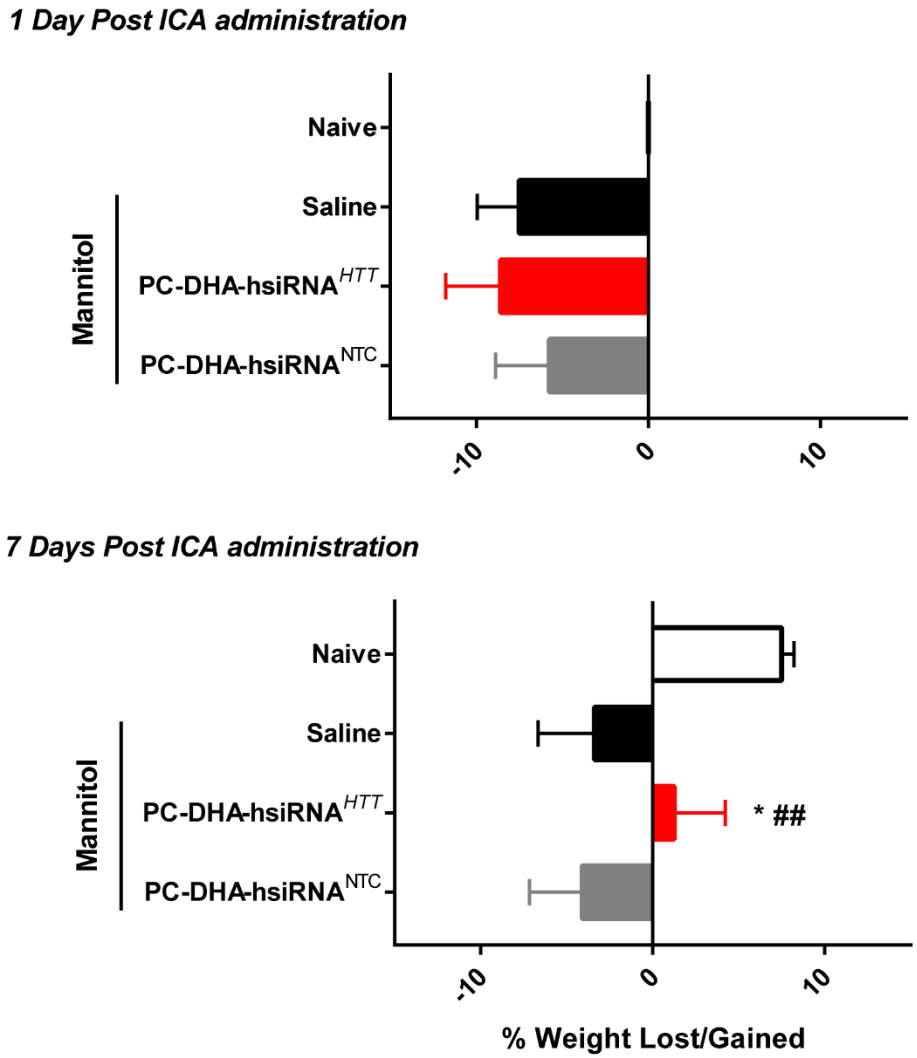

Figure S5. Percent change in body weight after transvascular delivery of PC-DHA-hsiRNAs by mannitol-induced blood-brain barrier disruption.

PC-DHA-hsiRNAs (16 mg/kg) or saline were administered through the right carotid artery after pre-treatment with mannitol. Animals were monitored for 7 days post-injection until they were euthanized for tissue collection. Percent loss or gain in body weight at 1 day (upper) and 7 days (lower). n = 3-7 animals/group, mean ± SD. One-way ANOVA with Tukey's post-hoc, *P<0.05 vs. Saline and ##P<0.01 vs. PC-DHA-hsiRNA^{NTC}.

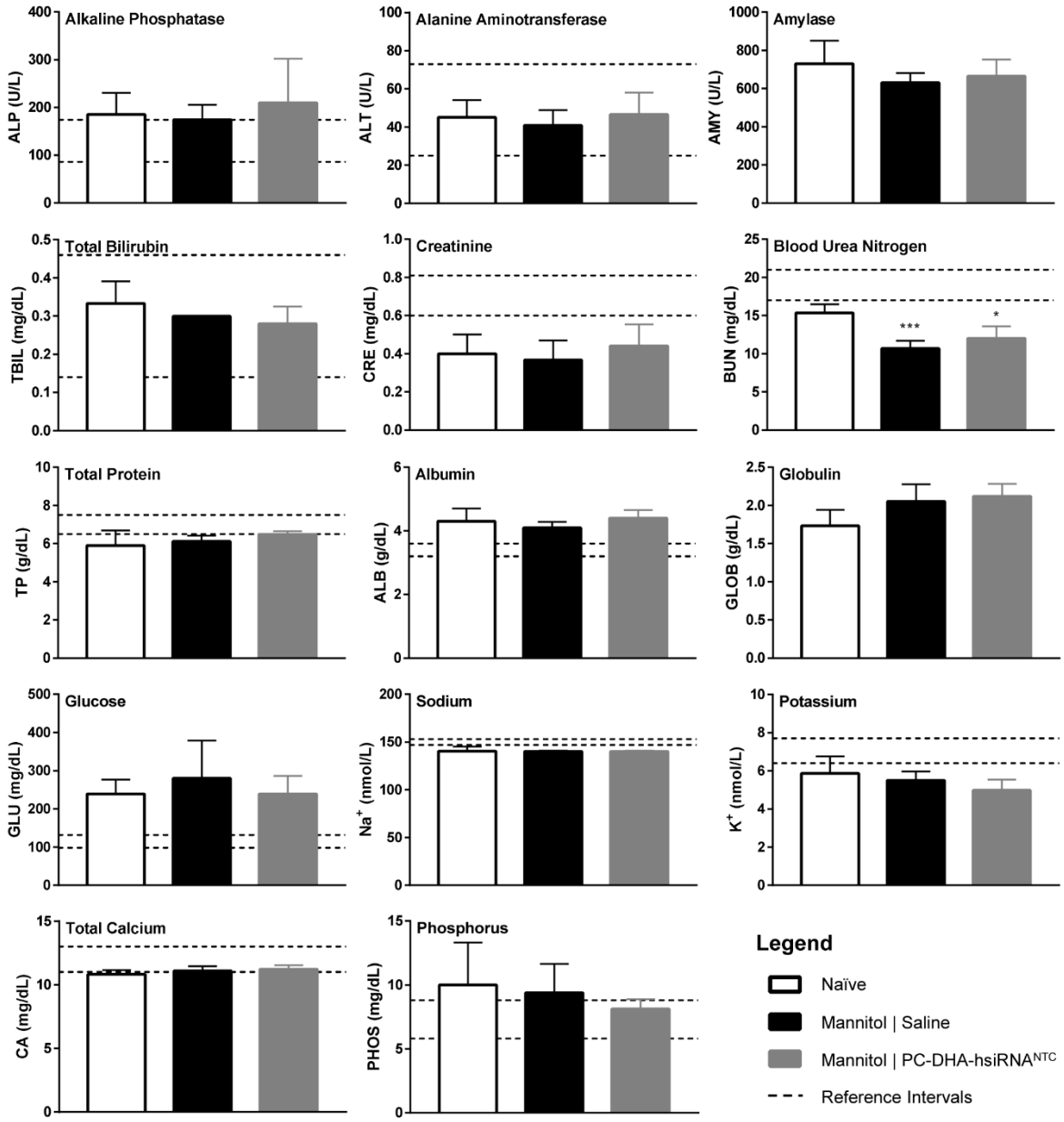

Figure S6. PC-DHA-hsiRNAs do not cause major acute systemic toxicities after mannitol-mediated transvascular delivery to the brain.

PC-DHA-hsiRNAs (16 mg/kg) or saline were administered through the right carotid artery after pre-treatment with mannitol. A comprehensive diagnostic blood chemistry profile of 14 biochemical markers was analyzed 7 days post-injection using a VetScan 2. Dashed lines indicate reference intervals reported in Fox JG et al. (2015) *Laboratory Animal Medicine*. n = 3-8 animals/group, mean ± SD. One-way ANOVA with Tukey's post-hoc, *P<0.05 and ***P<0.001.

Supplemental Methods

Optimization of intracarotid administrations

Male Sprague-Dawley rats (age 8-9 weeks, weight ~290 g) were cannulated using two different strategies for administration of 0.9% saline or 25% mannitol (Hospira, Cat. # NDC 0409-4031-01) solutions, followed by an infusion of Cy3-labelled asymmetric hydrophobic siRNAs (hsiRNA). hsiRNAs where conjugated to phosphocholine docosahexanoic acid (PC-DHA). The first approach consisted of direct administrations into the common carotid artery (CCA) performed by implanting a catheter in the right CCA to deliver 16 mg/kg Cy3-labelled PC-DHA-hsiRNA. The second approach consisted of indirect administrations conducted by implanting a catheter in the right external carotid artery (ECA) and positioning it to deliver 37 mg/kg Cy3-labelled PC-DHA-hsiRNA into the right CCA. After injections, catheters were removed and the respective arteries ligated. For other surgical details regarding anesthesia, catheters, volumes and rates of injection refer to materials and methods in the main text. Animals were euthanized 48 hours after injections and perfused with phosphate-buffered saline (PBS). Brains were removed and sliced using a rat brain matrix and fixed in 10% formalin overnight. Tissues were embedded in paraffin and sliced in 4 µm sections for assessment of biodistribution and toxicity.

TUNEL assay

For terminal deoxynucleotidyl transferase dUTP nick end labeling (TUNEL), 4 µm sections were obtained from paraffin-embedded tissues. Sections deparaffinized in xylene in 3 rounds of incubation 5 min/each. Samples were incubated in 100% ethanol for 5 min and this step repeated 2 times. Slides were treated in 95% ethanol for 5 min and this step also repeated 2 times. Sections were washed in deionized water for 5 min twice. Tissues were permeabilized using 500 µL of PBS Triton X-100 0.5% for 20 min and subsequently washed with PBS. 50 µL of TUNEL reaction mixture from the *in situ* cell death detection kit (Sigma Aldrich, Cat# 11684795910) was added to each slide and incubated for 1 hour at 37°C. Slides were washed with PBS twice for 5 min and stained with DAPI (1:10,000, Molecular probes, Cat. #D1306) for 2 min. Permafluor Mounting media (ThermoScientific, Cat. #TA-030-FM) was used to place glass coverslips, and slides left to dry at 4°C overnight protected from light. Imaging was carried out using a Leica DMi8 Fluorescent microscope fitted with a Hamamatsu C11440 ORCA-Flash 4.0 camera and a 40x objective. Images were acquired under the same light intensity settings and exposure times set individually for each channel.

Comprehensive Diagnostic Blood Chemistry Profiles

Naïve Sprague-Dawley rats or animals subjected to mannitol-mediated BBB disruption were euthanized 7 days post intracarotid administrations. Blood was collected from the right atrium into a sodium heparin tube and kept on ice or at 4 °C until analysis. Blood samples were loaded on a comprehensive diagnostic profile rotor (Abaxis, Cat. #500-0038) and analyzed through a VetScanVS2. Reference values for each of the blood chemistries were obtained from Fox, J.G. (2015) *Laboratory animal medicine*.